Inorg. Chem. **2007**, *46*, 756–766

Odd-Numbered Fe^{III} Complexes: Synthesis, Molecular Structure, Reactivity, and Magnetic Properties

Ayuk M. Ako,[†] Oliver Waldmann,*[,‡] Valeriu Mereacre,[†] Frederik Klöwer,[†] Ian J. Hewitt,[†] Christopher E. Anson,[†] Hans U. Güdel,[‡] and Annie K. Powell*[,†]

Institut für Anorganische Chemie der Universität Karlsruhe, Engesserstrasse Geb. 30.45, D-76128 Karlsruhe, Germany, and Department of Chemistry and Biochemistry, University of Bern, Freiestrasse 3, CH-3012 Bern, Switzerland

Received August 31, 2006

Three isostructural disklike heptanuclear Fe^{III} compounds of the general formula $[Fe^{III}_7(\mu_3\text{-}O)_3(L)_3(\mu\text{-}O_2CCMe_3)_6(\eta^1\text{-}O_2CCMe_3)_3(H_2O)_3]$, where L represents a di- or triethanolamine moiety, display a three-blade propeller topology, with the central Fe atom representing the axle or axis of the propeller. This motif corresponds to the theoretical model of a frustrated Heisenberg star, which is one of the very few solvable models in the area of frustrated quantum-spin systems and can, furthermore, be converted to an octanuclear cage for the case where L is triethanolamine to give $[Fe^{III}_8(\mu_4O)_3(\mu_4\text{-tea})(teaH)_3(O_2CCMe_3)_6(N_3)_3]\cdot{}^1/_2MeCN\cdot{}^1/_2H_2O$ or $[Fe^{III}_8(\mu_4O)_3(\mu_4\text{-tea})(teaH)_3(O_2CCMe_3)_6(SCN)_3]\cdot 2MeCN$ when treated with excess NaN_3 or NH_4SCN, respectively. The core structure is formally derived from that of the heptanuclear compounds by the replacement of the three aqua ligands by an {Fe(tea)} moiety, so that the 3-fold axis of the propeller is now defined by two central Fe^{III} atoms. Magnetic studies on two of the heptanulcear compounds established unequivocally $S = {}^5/_2$ spin ground state for these complexes, consistent with overall antiferromagnetic interactions between the constituent Fe^{III} ions.

Introduction

In the last few decades, the synthesis of polynuclear compounds of magnetic transition-metal ions[1] has become the focus of intense research activities because of their relevance to biological systems[2] and their potential as molecular species that can function as nanoscale magnetic particles or so-called single-molecule magnets, SMMs.[3] For example, the iron-storage protein ferritin and manganese clusters have been extensively studied as a biological prototype in the inorganic systems[4] and as models of the water-oxidizing complex in photosystem II,[5] respectively. The thoroughly studied $[Mn_{12}O_{12}(OAc)_{16}(H_2O)_4]$[3c] and $[Fe_8O_2(OH)_{12}(tacn)_6]Br$[3d] clusters respectively represent prototypes of Mn and Fe complexes showing SMM behavior.

Another reason for continued interest in the synthesis and study of polynuclear paramagnetic 3d metal clusters is the aesthetically pleasing nature of some of these species.[6] A particularly intriguing class are the so-called molecular ferric

* To whom correspondence should be addressed. E-mail: oliver.waldmann@iac.unibe.ch (O.W.), powell@aoc.uni-karlsruhe.de (A.K.P.). Tel: +49-721-608-2135 (A.K.P.). Fax: +49-721-608-8142 (A.K.P.).

† Institut für Anorganische Chemie der Universität Karlsruhe.

‡ University of Bern.

(1) Müller, A.; Peters, F.; Pope, M. T.; Gatteschi, D. *Chem. Rev.* **1998**, 239 and references cited therein.

(2) (a) Lippard, S. J. *Angew. Chem., Int. Ed. Engl.* **1988**, *27*, 344. (b) Pope, M. T.; Müller, A. *Angew. Chem., Int. Ed. Engl.* **1991**, *30*, 34. (c) Katsoulis, D. E. *Chem. Rev.* **1998**, *98*, 359.

(3) (a) Gatteschi, D.; Sessoli, R. *Angew. Chem., Int. Ed.* **2003**, *42*, 268. (b) Christou, G.; Gatteschi, D.; Hendrickson, D. N. *MRS Bull.* **2000**, *25*, 66. (c) Sessoli, R.; Gatteschi, D.; Caneschi, A.; Novak, M. A. *Nature* **1993**, *365*, 141. (d) Barr, A. L.; Debrunner, P.; Gatteschi, D.; Schulz, C. E.; Sessoli, R. *Europhys. Lett.* **1996**, *35*, 133.

(4) (a) Taft, K. L.; Delfs, C. D.; Papaefthymiou, G. C.; Foner, S.; Gatteschi, D.; Lippard, S. J. *J. Am. Chem. Soc.* **1994**, *116*, 823. (b) Crichton, R. R. *Angew. Chem., Int. Ed. Engl.* **1973**, *12*, 57. (c) Taft, K. L.; Papaefthymiou, G. C.; Lippard, S. J. *Science* **1993**, *259*, 1302.

(5) (a) Wieghardt, K. *Angew. Chem., Int. Ed. Engl.* **1994**, *33*, 725. (b) Debus, R. J. *Biochim. Biophys. Acta* **1992**, *1102*, 269. (c) Bruvig, G. W.; Thorp, H. H.; Crabtree, R. H. *Acc. Chem. Res.* **1991**, *24*, 311.

(6) (a) Tasiopoulos, A. J.; Vinslava, A.; Wernsdorfer, W.; Abboud, K. A.; Christou, G. *Angew. Chem., Int. Ed.* **2004**, *43*, 2117. (b) Low, D. M.; Jones, L. F.; Bell, A.; Brechin, E. K.; Mallah, T.; Rivière, E.; Teat, S. J.; McInnes, E. J. L. *Angew. Chem., Int. Ed.* **2004**, *42*, 3781. (c) Langley, S.; Helliwell, M.; Raftery, J.; Tolis, E. I.; Winpenny, R. E. P. *Chem. Commun.* **2004**, 142. (d) Jones, L. F.; Brechin, E. K.; Collison, D.; Harrison, A.; Teat, S. J.; Wernsdorfer, W. *Chem. Commun.* **2002**, 2974. (e) Paine, T. K.; Rentschler, E.; Weyhermüller, T.; Chaudhuri, P. *Eur. J. Inorg. Chem.* **2003**, 3167. (f) Overgaard, J.; Iversen, B. B.; Palii, S. P.; Timco, G. A.; Gerbeleu, N. V.; Larsen, F. K. *Chem.—Eur. J.* **2002**, *8*, 2775. (g) Abedin, T. S. M.; Thompson, L. K.; Miller, D. O.; Krupicka, E. *Chem. Commun.* **2003**, 708. (h) Murugesu, M.; Anson, C. E.; Powell, A. K. *Chem. Commun.* **2002**, 1054. (i) Abati, G. L.; Cornia, A.; Fabretti, A. C.; Caneschi, A.; Gatteschi, D. *Inorg. Chem.* **1998**, *37*, 1430.

10.1021/ic061650s CCC: $37.00
Published on Web 01/05/2007

wheels with nuclearity Fe_x ranging from 6 to 18 Fe^{III} ions.[7,8] The magnetization of the ferric wheels exhibits steplike field dependencies at low temperatures due to the importance of finite-size quantum effects.[4a,9] Initially, these systems were regarded as ideal models for the finite-size version of the linear 1D Heisenberg chain, but subsequently it was realized that their magnetic behavior at low temperatures is best described by a quantized rotation of the Néel vector and, hence, is more similar to that of 2D and 3D materials.[10] Moreover, quantum phenomena such as Néel-vector tunneling were demonstrated.[11] Because of the rich physics observed in molecular wheels and a promising potential for quantum computing,[12] this class of molecules has become increasingly important.

Alkoxo ligands, for example, N-substituted diethanolamines, have been employed extensively in the construction of hybrid organic−inorganic clusters because of their versatile bridging modes, with subtle changes in the reaction conditions resulting in the formation of unexpected and beautiful structures such as cyclic polymetallic clusters.[13] Along these lines, Saalfrank and co-workers reported on the template-mediated self-assembly of six- and eight-membered iron coronates $\{Na[Fe_6(tea)_6]\}Cl$ (**6**) and $\{Cs[Fe_8(tea)_8]\}Cl$ (**7**), obtained from the reaction of triethanolamine ($teaH_3$) with $FeCl_3$, NaH, or Cs_2CO_3.[7b] In addition, they reported on a wide range of six-membered iron coronands obtained from the reaction of N-substituted diethanolamines with $FeCl_3$ and CaH_2 in tetrahydrofuran.[14] Recently, using Schiff base ligands with an alkyl alcohol group, Oshio and co-workers reported a high spin ($S = {}^{29}/_{2}$) hepatanuclear mixed-valent $Fe^{II,III}$ wheel, which showed SMM behavior.[15]

Chart 1. $teaH_3$, H_3L^1 (Left), $bdeaH_2$, H_2L^2 (Center), and Phdea, H_2L^3 (Right)

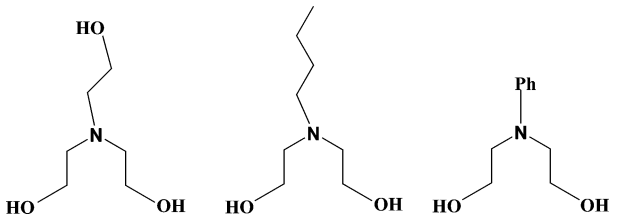

In contrast to the large number of even-numbered Fe^{III} wheels known, which have been obtained from the reaction of suitable chelating ligands with preformed oxo-centered Fe^{III} triangles,[7e,16] odd-numbered, disklike, all-Fe^{III} complexes are rare.[17] Such Fe^{III} complexes are interesting not only from a chemical and structural perspective but also because elucidation of their magnetic properties and spin topologies should help in understanding the magnetic properties of larger ferric systems. The arrangement in such a heptanuclear structure can be regarded as a ring comprising an even number of Fe^{III} ions with an additional central Fe^{III} ion, which can be predicted to allow for strong quantum-spin frustration effects due to competing nearest-neighbor exchange interaction paths. In fact, the exchange-coupling situation realized in such clusters bears a close analogy to the so-called frustrated Heisenberg star introduced by Richter and Voigt as a rare example of an exactly solvable quantum-spin model with frustration.[18]

Hence, as an extension of our recent work on the reaction of diethanolamine ligands with preformed oxo-centered Fe^{III} triangles,[19] we report here on the reaction of $teaH_3$, *N*-butyldiethanolamine ($bdeaH_2$), and phenyldiethanolamine (Phdea) (Chart 1) with $[Fe_3O(O_2CCMe_3)_6(H_2O)_3](O_2CCMe_3)$ in the presence of metal(II) pivalates (metal = nickel, copper) or $Ni(OAc)_2{\cdot}4H_2O$, which results in the formation of the heptanuclear Fe^{III} clusters **1**−**3**, respectively, in high yields. The crystal structures of compounds **1**−**3** and the magnetic properties of complexes **1** and **2** are discussed. We report here also the structure of the octanuclear clusters $[Fe^{III}_8(\mu_4O)_3(\mu_4\text{-tea})(teaH)_3(O_2CCMe_3)_6(N_3)_3]$ (**4**) and $Fe^{III}_8(\mu_4O)_3(\mu_4\text{-tea})(teaH)_3(O_2CCMe_3)_6(SCN)_3]$ (**5**) and the mononuclear complex $[Ni(teaH_3)_2](O_2CCMe_3)_2$ (**6**), obtained from the reaction of **1** with excess NaN_3, or NH_4SCN, and as a byproduct of the synthetic procedure used for **1**, respectively.

(7) (a) Sydora, O. L.; Woleczanski, P. T.; Lobkovsky, E. B. *Angew. Chem., Int. Ed.* **2003**, *42*, 2685 and references cited therein. (b) Saalfrank, R. W.; Bernt, I.; Uller, E.; Hampel, F. *Angew. Chem., Int. Ed. Engl.* **1997**, *36*, 2482. (c) Caneschi, A.; Cornia, A.; Fabretti, A. C.; Gatteschi, D. *Angew. Chem., Int. Ed.* **1999**, *38*, 1295. (d) Watton, S. P.; Fuhrmann, P. L.; Pence, E.; Caneschi, A.; Cornia, A.; Abbati, G. L.; Lippard, J. S. *Angew. Chem., Int. Ed. Engl.* **1997**, *36*, 2774. (e) Cañada-Vilalta, C.; O'Brien, T. A.; Brechin, E. K.; Pink, M.; Davidson, E. R.; Christou, G. *Inorg. Chem.* **2004**, *43*, 5505. (f) Jones, L. F.; Low, D. M.; Helliwell, M.; Raftery, J.; Collison, D.; Aromí, G.; Cano, J.; Mallah, T.; Wernsdorfer, W.; Brechin, E. K.; McInnes, E. J. L. *Polyhedron* **2006**, *25*, 325.

(8) Yao, H. C.; Wang, J. J.; Ma, Y. S.; Waldmann, O.; Du, W. X.; Song, Y.; Li, Y. Z.; Zheng, L. M.; Decurtins, S.; Xin, X. Q. *Chem. Commun.* **2006**, 1745.

(9) (a) Cornia, A.; Affronte, M.; Jansen, A. G. M.; Abbati, G. L.; Gatteschi, D. *Angew. Chem., Int. Ed.* **1999**, *38*, 2264. (b) Waldmann, O.; Schülein, J.; Koch, R.; Müller, P.; Bernt, I.; Saalfrank, R. W.; Andres, H. P.; Güdel, H. U.; Allenspach, P. *Inorg. Chem.* **1999**, *38*, 5879. (c) Waldmann, O.; Koch, R.; Schromm, S.; Schülein, J.; Müller, P.; Bernt, I.; Saalfrank, R. W.; Hampel, F.; Balthes, E. *Inorg. Chem.* **2001**, *40*, 2986.

(10) (a) Waldmann, O. *Phys. Rev. B* **2002**, *65*, 024424. (b) Waldmann, O.; Guidi, T.; Carretta, S.; Mondelli, C.; Dearden, A. L. *Phys. Rev. Lett.* **2003**, *91*, 237202. (c) Waldmann, O. *Coord. Chem. Rev.* **2005**, *249*, 2550.

(11) Waldmann, O.; Dobe, C.; Mutka, H.; Furrer, A.; Güdel, H. U. *Phys. Rev. Lett.* **2005**, *95*, 057202.

(12) (a) Troiani, F.; Affronte, M.; Carretta, S.; Santini, P.; Amoretti, G. *Phys. Rev. Lett.* **2005**, *94*, 190501. (b) Troiani, F.; Ghirri, A.; Affronte, M.; Carretta, S.; Santini, P.; Amoretti, G.; Piligkos, S.; Timco, G.; Winpenny, R. E. P. *Phys. Rev. Lett.* **2005**, *94*, 207208.

(13) (a) Caneschi, A.; Cornia, A.; Lippard, S. J. *Angew. Chem., Int. Ed. Engl.* **1995**, *34*, 467. (b) Watton, S. P.; Fuhrmann, P.; Pence, L. E.; Caneschi, A.; Cornia, A.; Abbati, G. L.; Lippard, S. J. *Angew. Chem., Int. Ed. Engl.* **1997**, *36*, 2774. (c) Abbati, G. L.; Cornia, A.; Fabretti, A. C.; Caneschi, A.; Gatteschi, D. *Inorg. Chem.* **1998**, *37*, 3759. (d) Dearden, A. L.; Parsons, S.; Winpenny, R. E. P. *Angew. Chem., Int. Ed.* **2001**, *40*, 151.

(14) Saalfrank, R. W.; Deutscher, C.; Sperner, S.; Nakajima, T.; Ako, A. M.; Uller, E.; Hampel, F.; Heinemann, F. W. *Inorg. Chem.* **2004**, *43*, 4372.

(15) Oshio, H.; Hoshino, N.; Ito, T.; Nakano, M.; Renz, F.; Gütlich, P. *Angew. Chem., Int. Ed.* **2003**, *42*, 223 and references cited therein.

(16) (a) Murugesu, M.; Abboud, K. A.; Christou, G. *Dalton Trans.* **2003**, 4552. (b) Jones, L. F.; Jensen, P.; Moubaraki, B.; Cashion, J.; Berry, K. J.; Murray, K. S. *Dalton Trans.* **2005**, 3344.

(17) While this manuscript was in preparation, Murray et al. reported the structure of compound **1**: Jones, L. F.; Jensen, P.; Moubaraki, B.; Berry, K. J.; Boas, J. F.; Pilbrow, J. R.; Murray, K. S. *J. Mater. Chem.* **2006**, *16*, 2690.

(18) (a) Richter, J.; Voigt, A. *J. Phys. A: Math. Gen.* **1994**, *27*, 1139. (b) Richter, J.; Voigt, A.; Krüger, S. E.; Gross, C. *J. Phys. A: Math. Gen.* **1996**, *29*, 825.

(19) Ako, A. M.; Mereacre, V.; Hewitt, I. J.; Clérac, R.; Lecren, L.; Anson, C. E.; Powell, A. K. *J. Mater. Chem.* **2006**, *16*, 2579.

Experimental Section

General Procedures. Unless otherwise stated, all reagents were obtained from commercial sources and were used as received, without further purification. $[Fe_3O(O_2CCMe_3)_6(H_2O)_3](O_2CCMe_3)$,[20] $[Cu_2(\mu\text{-}OH_2)(O_2CCMe_3)_4(HO_2CCMe_3)_4]$, and $[Ni_2(\mu\text{-}OH_2)(O_2CCMe_3)_4(HO_2CCMe_3)_4]$[21] were synthesized as described elsewhere. All reactions were carried out under aerobic conditions.

The elemental analyses (CHN) were performed using an Elementar Vario EL analyzer. Fourier transform IR spectra were measured on a Perkin-Elmer Spectrum One spectrometer with samples prepared as KBr disks.

X-ray Crystallography. Data were collected at 100 K on a Bruker SMART Apex CCD diffractometer (**1**−**4** and **6**) or at 150 K on a Stoe IPDS II area detector diffractometer (**5**) using graphite-monochromated Mo Kα radiation. Crystallographic details and details of the data collection are summarized in Table 1. Semiempirical absorption corrections were made using *SADABS*[22a] (**1**−**4**) or *XPREP* in *SHELXTL*[22b] (**5** and **6**). The structures were solved using direct methods, followed by full-matrix least-squares refinement against F^2 (all data) using *SHELXTL*.[22b] Anisotropic refinement was used for all ordered non-H atoms; organic H atoms were placed in calculated positions, while coordinates of hydroxo H atoms were refined.

Magnetic Measurements. The magnetic susceptibility versus temperature and the magnetization curves at low temperatures were measured with a Quantum Design SQUID magnetometer MPMS-XL. The samples used for the magnetic measurements were prepared in three different ways. *Procedure A:* Polycrystalline material was prepared by drying crystals under ambient conditions. About 10 mg of material was encapsulated in Saran foil, put into a plastic straw, and held in place with a cotton thread. The weight of the sample could be accurately determined to within 0.1%. The magnetic data were corrected for the background due to the Saran foil. *Procedure B:* A total of 20−40 crystals were taken out of the mother liquor, put directly into Apiezon grease, and "stirred". Then as much grease as possible was removed, and the sample was weighed (typically 2 mg). *Procedure C:* A single crystal was taken out of the mother liquor and then treated as it was in procedure B (ca. 1.2 mg).

Because of the unknown amount of grease left over in procedures B and C, the measured weight of a sample provides an upper limit for the actual weight of the magnetic material, but the accuracy is estimated to better than 10%. Also, the magnetic data cannot be corrected for the diamagnetic (temperature-independent) contribution of the grease; its contribution is an estimated 5% at 300 K but is completely negligible at temperatures below 10 K. The advantage of these procedures is that they avoid potential problems with decomposition and typically minimize contamination by magnetic impurities.

Synthesis of $[Fe^{III}_7(\mu_3\text{-}O)_3(teaH)_3(\mu\text{-}O_2CCMe_3)_6(\eta^1\text{-}O_2CCMe_3)_3(H_2O)_3]$ (1). To a stirred solution of $[Ni_2(\mu\text{-}OH_2)(O_2CCMe_3)_4(HO_2CCMe_3)_4]$ (0.09 g, 0.1 mmol) and $[Fe_3O(O_2CCMe_3)_6](O_2CCMe_3)$ (0.1 g, 0.1 mmol) in MeCN (20 mL) was gradually added a solution of triethanolamine ($teaH_3$; H_3L^1; 0.3 g, 2 mmol) in MeCN (5 mL). The resulting dark-brown solution was stirred under ambient conditions for a further 1 h, filtered, and then allowed to stand undisturbed in a sealed vial. Dark-brown hexagonal prisms of **1** suitable for X-ray crystallography were obtained overnight. The crystals of **1** were maintained in the mother liquor for X-ray crystallography or collected by filtration, washed with Et_2O, and dried in a slow flow of N_2. Yield: 30.2 mg, 40% based on Fe. Anal. Calcd for $C_{63}H_{126}Fe_7N_3O_{33}$ (found): C, 41.02 (41.21); H, 6.88 (6.69); N, 2.27 (2.22). Selected IR data (KBr disk, cm^{-1}): 3447 (b), 2959 (s), 2870 (s), 1567 (s), 1484 (s), 1423 (s), 1359 (m), 1228 (s), 1103 (s) 1077 (s), 1039 (s), 921 (s), 789 (s), 685 (w), 604 (w), 495 (m), 435 (w). The same product is obtained in ca. 30% yield if $[Cu_2(\mu\text{-}OH_2)(O_2CCMe_3)_4(HO_2CCMe_3)_4]$ is employed in place of $[Ni_2(\mu\text{-}OH_2)(O_2CCMe_3)_4(HO_2CCMe_3)_4]$. Crystals of these were obtained after 48 h. The material was identified by IR spectral comparison with the title compound.

A week after the isolation of **1**, a few blue crystals were collected from the mother liquor and identified by an X-ray structure analysis (see the Supporting Information) to be the mononuclear complex $[Ni(teaH_3)_2](O_2CCMe_3)_2$ (**6**). Anal. Calcd for $C_{22}H_{48}N_2NiO_{10}$ (found): C, 47.24 (47.32); H, 8.65 (8.54); N, 5.01 (5.22). Selected IR data (KBr disk, cm^{-1}): 3348 (b), 2974 (s), 2880 (m), 2452 (b), 2068 (b), 1912 (b), 1527 (b), 1384 (w), 1225 (s), 115 (s), 1062 (m), 1002 (s), 903 (s), 790 (s), 601 (s), 429 (w). No corresponding copper byproduct was isolated when copper pivalate was employed.

Synthesis of $[Fe^{III}_7(\mu_3\text{-}O)_3(bdea)_3(\mu\text{-}O_2CCMe_3)_6(\eta^1\text{-}O_2CCMe_3)_3(H_2O)_3]$ (2). The synthesis was similar to that of **1** but replacing $[Ni_2(\mu\text{-}OH_2)(O_2CCMe_3)_4(HO_2CCMe_3)_4]$ with $Ni(OAc)_2{\cdot}4H_2O$ and $teaH_3$ (H_3L^1) with *N*-butyldiethanolamine ($bdeaH_2$; H_2L^2). Orange crystals of **2** were obtained after 72 h, washed with Et_2O, and dried in a slow flow of N_2. Yield: 24 mg, 30% based on Fe. Anal. Calcd for $C_{69.5}H_{138}Fe_7N_3O_{30}$ (found): C, 43.42 (43.18); H, 7.24 (7.43); N, 2.19 (2.21). Selected IR data (KBr disk, cm^{-1}): 3519 (b), 2960 (s), 2927 (m), 2866 (s), 1575 (b, s), 1483 (s), 1423 (s), 1407 (m), 1368 (m), 1355 (m), 1103 (s), 1063 (s), 1049 (s), 1006 (s), 906 (s), 785 (s), 680 (b, s), 621 (s), 438 (w). The corresponding mononuclear Ni byproduct was obtained after compound **2** was isolated and the mother liquor was allowed to stand for a further 2 days.

Synthesis of $[Fe^{III}_7(\mu_3\text{-}O)_3(Phdea)_3(\mu\text{-}O_2CCMe_3)_6(\eta^1\text{-}O_2CCMe_3)_3(H_2O)_3]$ (3). The synthesis was similar to that of **1** but replacing $[Ni_2(\mu\text{-}OH_2)(O_2CCMe_3)_4(HO_2CCMe_3)_4]$ with $Ni(OAc)_2{\cdot}4H_2O$ and $teaH_3$ (H_3L^1) with phenyldiethanolamine (Phdea; H_2L^3). Orange crystals of **3** were obtained after 1 week, washed with Et_2O, and dried in a slow flow of N_2. Yield: 27.8 mg, 35% based on Fe. Anal. Calcd for $C_{75}H_{126}Fe_7N_3O_{30}$ (found): C, 46.42 (46.38); H, 6.54 (6.45); N, 2.17 (2.21). Selected IR data (KBr disk, cm^{-1}): 3509 (b), 2960 (s), 2927 (m), 2858 (m), 1571 (s), 1483 (s), 1425 (s), 1406 (s), 1376 (m), 1355 (s), 1228 (s), 1107 (m), 1059 (w), 1049 (s), 1009 (w), 925 (w), 788 (w), 697 (m), 677 (s), 602 (s), 591 (s), 439 (w).

Synthesis of $[Fe^{III}_8(\mu_4O)_3(\mu_4\text{-}tea)(teaH)_3(O_2CCMe_3)_6(N_3)_3]$ (4). The synthesis was similar to that of **1**, however, in the presence of NaN_3 (0.07 g, 1 mmol). The reaction mixture was stirred at room temperature for 2 h to yield an orange solution, then filtered, and allowed to evaporate slowly at room temperature. Brown crystals of **4** were obtained after 48 h, washed with Et_2O, and dried in a slow flow of N_2. Yield: 28 mg, 40% based on Fe. Anal. Calcd for $C_{55}H_{107.5}Fe_8N_{413.5}O_{27.5}$ (found): C, 35.81 (35.67); H, 5.85 (5.96); N, 10.25 (10.14). Selected IR data (KBr disk, cm^{-1}): 3453 (b), 2959 (s), 2903 (m), 2873 (m), 2060 (s), 1575 (b, s), 1484 (s), 1426 (s), 1361 (w), 1227 (s), 1087 (m), 1075 (m), 1039 (w), 1004 (w), 909 (s), 786 (s), 603 (b), 425 (w). The same compound can be obtained directly by refluxing compound **1** with excess NaN_3 in

(20) Wilson, C.; Iversen, B. B.; Overgaard, J.; Larsen, F. K.; Wu, G.; Palii, S. P.; Timco, G. A.; Gerbeleu, N. V. *J. Am. Chem. Soc.* **2000**, *122*, 11370.

(21) Chaboussant, G.; Basler, R.; Güdel, H.-U.; Ochsenbein, S.; Parkin, A.; Parsons, S.; Rajaraman, G.; Sieber, A.; Smith, A. A.; Timco, G. A.; Winpenny, R. E. P. *Dalton Trans.* **2004**, 2758.

(22) (a) Sheldrick, G. M. *SADABS (the Siemens Area Detector Absorption Correction)*; University of Göttingen: Göttingen, Germany, 1996. (b) Sheldrick, G. M. *SHELXTL*, version 5.1; Bruker AXS, Inc.: Madison, WI, 1997.

Table 1. Crystallographic Data and Structure Refinement for Complexes **1**−**6**

	1	**2**	**3**
formula	$C_{63}H_{126}Fe_7N_3O_{33}$	$C_{69.5}H_{138}ClFe_7N_3O_{30}$	$C_{75}H_{126}Fe_7N_3O_{30}$
M_r	1844.62	1922.23	1940.74
cryst size [mm]	0.27 × 0.25 × 0.24	0.28 × 0.22 × 0.18	0.26 × 0.17 × 0.17
shape	hexagonal prism	block	block
color	dark brown	orange	orange
cryst syst	trigonal	monoclinic	monoclinic
space group	*P*31*c*	*C*2/*c*	$P2_1/n$
T [K]	100	100	100
a [Å]	15.5804(8)	63.351(3)	10.6609(5)
b [Å]	15.5804(8)	10.4329(5)	31.5950(14)
c [Å]	20.8694(11)	31.4090(16)	27.2343(11)
α [deg]	90	90	90
β [deg]	90	115.078(1)	90.120(1)
γ [deg]	120	90	90
V [Å^3]	4387.3(4)	18802.3(16)	9173.3(7)
Z	2	8	4
ρ_{calcd} [g cm^{-3}]	1.523	1.358	1.405
μ(Mo Kα) [mm^{-1}]	1.202	1.150	1.151
F(000)	1942	8120	4076
reflns collected	16 786	46 786	46 053
unique reflns	5060	21 285	20 567
R_{int}	0.0295	0.0329	0.0253
reflns obsd [$I > 2\sigma$(I)]	4823	14323	14887
parameters/restraints	326/4	1044/24	1087/10
GOF on F^2	1.051	0.986	1.036
R1 [$I > 2\sigma(I)$]	0.0338	0.0380	0.0457
wR2 (all data)	0.0869	0.0822	0.1380
largest residuals [e Å^{-3}]	+0.90/−0.33	+1.08/−0.56	+1.5/−0.70
CCDC number	618914	618915	618916

	4	**5**	**6**
formula	$C_{55}H_{107.5}Fe_8N_{13.5}O_{27.5}N_3$	$C_{61}H_{111}Fe_8N_9O_{27}S_3$	$C_{22}H_{48}N_2NiO_{10}$
M_r	1844.84	1945.57	559.33
cryst size [mm]	0.34 × 0.28 × 0.25	0.32 × 0.21 × 0.13	0.37 × 0.18 × 0.08
shape	octahedron	block	plate
color	brown	brown	pale blue
cryst syst	monoclinic	monoclinic	monoclinic
space group	$P2_1/c$	*C*2/*c*	$P2_1/n$
T [K]	100	150	100
a [Å]	23.6121(8)	55.495(2)	12.9960(14)
b [Å]	15.0975(5)	15.4971(9)	6.9495(7)
c [Å]	44.6731(14)	21.1361(9)	16.1600(17)
α [deg]	90	90	90
β [deg]	94.523(1)	110.992	102.368(2)
γ [deg]	90	90	90
V [Å^3]	15875.6(9)	16969.9(14)	1425.6(3)
Z	8	8	2
ρ_{calcd} [g cm^{-3}]	1.544	1.523	1.303
μ(Mo Kα) [mm^{-1}]	1.501	1.477	0.732
F(000)	7680	8096	604
reflns collected	79 377	56 154	6904
unique reflns	35 692	17 443	3196
R_{int}	0.0391	0.0458	0.0268
reflns obsd [$I > 2\sigma$(I)]	20 937	11 437	2386
parameters/restraints	1851/11	972/10	172/0
GOF on F^2	0.978	1.012	1.002
R1 [$I > 2\sigma(I)$]	0.0504	0.0516	0.0299
wR2 (all data)	0.1276	0.1254	0.0649
largest residuals [e Å^{-3}]	+1.92/−1.18	+0.74/−0.81	+0.56/−0.29
CCDC number	618917	618918	618919

CH_2Cl_2/MeOH (1: 3) for 2 h. Crystals of **4** were obtained in quantitative yield after 24 h. The product was identified using IR spectroscopy. Complex **5** was synthesized in a manner similar to that of **4**, except that NH_4SCN was used in place of NaN_3.

Results and Discussion

Synthesis. Reaction of a 10-fold excess of H_2L^1 with $[Fe_3O(O_2CCMe_3)_6(H_2O)_3](O_2CCMe_3)$ and $[Ni_2(\mu\text{-}OH_2)(O_2CCMe_3)_4(HO_2CCMe_3)_4]$ in MeCN afforded dark-brown crystals of **1** in 40% yield. Alternatively, complex **1** was obtained in 30% yield when $[Cu_2(\mu\text{-}OH_2)(O_2CCMe_3)_4(HO_2CCMe_3)_4]$ was used in place of the Ni analogue. Reaction of H_2L^2 with $Ni(OAc)_2{\cdot}4H_2O$ and $[Fe_3O(O_2CCMe_3)_6(H_2O)_3](O_2CCMe_3)$ in MeCN gave orange blocks of the heptanuclear cluster $\mathbf{2}{\cdot}{}^1/_2CH_2Cl_2$ in 25% yield, while a similar reaction using H_2L^3 as the ligand gave **3** in 35% yield (Scheme 1).

Compounds **1**−**3** can be prepared directly from the reaction of the corresponding ligands with the Fe_3O pivalate

Scheme 1. Synthetic Pathways for the Synthesis of Compounds **1**−**5**[a]

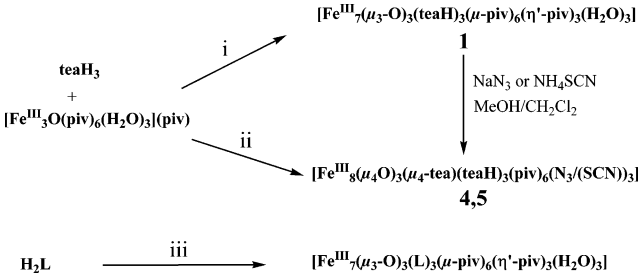

[a] Reaction conditions: (i) $[M_2(\mu\text{-}OH_2)(piv)_4(pivH)_4]$ (M = Ni, Cu), MeCN; (ii) $[Ni_2(\mu\text{-}OH_2)(piv)_4(pivH)_4]/NaN_3$ (**4**) or -/NH_4SCN (**5**), MeCN; (iii) $Ni(OAc)_2{\cdot}4H_2O$, MeCN [L = bdea (**2**), Phdea (**3**)].

triangle. However, the products are obtained after an extended reaction time and in lower yields, as was recently reported for compound **1**.[17] To our knowledge, complex **3** represents the first high-nuclearity Phdea-based compound reported so far. Elemental analysis, IR, and single-crystal X-ray crystallography (see the Experimental Section) were used to characterize the compounds. Contrary to what we expected, the M^{II} ions are not incorporated in the products. However, a mononuclear Ni complex (**6**) was isolated as a byproduct when nickel pivalate or nickel acetate was used in conjunction with the Fe^{III} source. Although no such crystalline byproduct was obtained when copper(II) pivalate was employed, we conjecture from the nature of the crystalline Ni complex formed as the byproduct that these M^{II} starting materials provide a means of driving the reaction equilibria toward the side of the products through the favorable chelate and ligand-field effects in forming M^{II} complexes with the ethanolamine ligands.

Previous work on the complex formation of Fe^{III} with amino alcohol ligands includes a similar reaction using $teaH_3$,[16a] diisopropanolamine,[16b] and phosphonate ligands[23] or 2-(2-hydroxyethyl)pyridine[7e] with $[Fe_3O(O_2CR)_6(H_2O)_3]X$ (R = Ph, $CCMe_3$; X = O_2CCMe_3, O_2CPh, NO_3), which result in the formation of even-numbered hexa- or octanuclear Fe^{III} clusters that have $S = 0$ spin ground states.[7e,12] Equally, the reaction of the tripodal ligand 1,1,1-tris(hydroxymethyl)-ethane (H_3thme) with $[Fe_3O(O_2CCMe_3)_6(H_2O)_3](X)$ (X = O_2CCMe_3, Cl) under solvothermal conditions led to octanuclear $[Fe^{III}_8(O_2CCMe_3)_{12}(thme)_4]$ or nonanuclear $[Fe^{III}_9O_4(O_2CCMe_3)_{13}(thme)_2]$ clusters.[7f] Meanwhile, the reaction of benzotriazole (btah) with $[Fe_3O(O_2CR)_6(H_2O)_3]Cl$ in MeOH under the same solvothermal conditions gave the tetradecametallic high-spin $S = 23$ Fe^{III} cluster $[Fe_{14}(bta)_6O6(OMe)_{18}Cl_6]$.[6b] Other groups have also demonstrated that diethanolamine ligands form wheel-shaped structures. In this regard, neutral iron coronands $[Fe_6X_6L_6]$ or $[Fe_6L_6]$ (L = N-substituted diethanolamine; X = Cl, F) obtained from the reaction of diethanolamines with simple metal salts (FeX_3) have been reported.[24,25] Furthermore, this class of ligands recently has been used to assemble an unprecedented high-nuclearity cluster, consisting of 22 Fe^{III} ions, the largest homometallic Fe cluster reported to date.[26] Other high-nuclearity Fe^{III} complexes with non-wheel-like structures and odd numbers of Fe centers include, for example, the Fe_{11} cluster with an $S = {}^{11}/_2$ spin ground state, reported by McInnes et al.,[7f] and the Fe_{17} and Fe_{19} clusters with $S = {}^{25}/_2$ and ${}^{33}/_2$ ground states.[27] Statistical analysis of recent reports of Fe^{III} clusters obtained from preformed oxo-centered Fe triangles as a source of Fe^{III} ions shows that more even-numbered clusters, generally with $S = 0$, have been obtained than odd-numbered Fe^{III} clusters.

Compound **1** lends itself to further elaboration, for example, replacement of terminal pivalates or H_2O molecules with *pseudo*halides. Indeed, introducing excess NaN_3 or NH_4-SCN into the reaction mixture that produced **1** resulted in the isolation of the octanuclear clusters **4** or **5**, respectively, in high yields. Similarly, when crystalline material obtained from the synthesis of **1** was treated directly with excess NaN_3 or NH_4SCN, compounds identical with **4** or **5** (as established by IR spectra) were obtained in quantitative yield. The IR spectra of **4** and **5** exhibit a very strong absorption at 2060 or 2062 cm^{-1} corresponding to the azido as well as thiocyanate asymmetric vibrations,[28] respectively. It is noteworthy that heptanuclear Fe^{III}_7 clusters with different core topologies have been reported, obtained from the reaction of cyclohexenephosphonic acid (hydrothermally)[29] or phenylphosphonate ligands (at ambient conditions)[24] with preformed iron(III) carboxylate triangles $[Fe_3O(O_2CR)_6(H_2O)_3]X$ (R = Ph, Me; X = Cl, NO_3, $PhCO_2^-$). To our knowledge, the core topology shown by **1**−**3** is rare for odd-numbered Fe^{III} clusters obtained via oxo-centered Fe^{III} triangles as a source of Fe^{III} ions.[17]

Description of Crystal Structures of 1−3. Complexes **1**−**3** are analogous, differing only in the nature of the side arm of the ligand, and are among the first examples of this disklike heptanuclear motif in all-ferric form. They crystallize in the space groups *P*31*c* for **1**, *C*2/*c* for **2**, and $P2_1/n$ for **3**, with the Fe_7 molecules on general positions. The structure for **2** is shown in Figure 1, while selected interatomic distances and angles are listed in Table 2. Varying the side arm of the diethanolamine ligands, ethanol (for **1**), *n*-butyl (for **2**), and the rigid aromatic ring (for **3**) clearly has little impact on the way the ligands associate in the Fe^{III} clusters, and the driving force for the arrangement of the metal ions in the complexes is presumably the bite of the ONO donor set of the ligands as well as the associated pivalates and H_2O molecules. Contrary to what might have been anticipated, the pendent ethanol arm of $teaH_3$ is not implicated in the coordination of the ligand through its supplementary donor O atom of the side arm. Hence, $teaH_3$ behaves essentially as a tridentate ligand and not a tetradentate ligand. The core of

(23) Tolis, E. I.; Helliwell, M.; Langley, S.; Raftery, J.; Winpenny, R. E. P. *Angew. Chem., Int. Ed.* **2003**, *42*, 3804.
(24) Rumberger, E. M.; Zakharov, L. N.; Rheingold, A. L.; Hendrickson, D. N. *Inorg. Chem.* **2004**, *43*, 6531.
(25) Koizumi, S.; Nihei, M.; Nakano, M.; Oshio, H. *Inorg. Chem.* **2005**, *44*, 1208.
(26) Foguet-Albiol, D.; Abboud, K. A.; Christou, G. *Chem. Commun*. **2005**, 4282.
(27) Powell, A. K.; Heath, S. L.; Gatteschi, D.; Pardi, L.; Sessoli, R.; Spina, G.; Del Giallo, F.; Pieralli, F. *J. Am. Chem. Soc.* **1995**, *117*, 2491.
(28) (a) Barandika, M. G.; Cortés, R.; Lezama, L.; Urtiaga, M. K.; Arriortua, M. I.; Rojo, T. *J. Chem. Soc., Dalton Trans.* **1999**, 2971.
(29) Yao, H.-C.; Li, Y.-Z.; Zheng, L.-M.; Xin, X.-Q. *Inorg. Chim. Acta* **2005**, *358*, 2523.

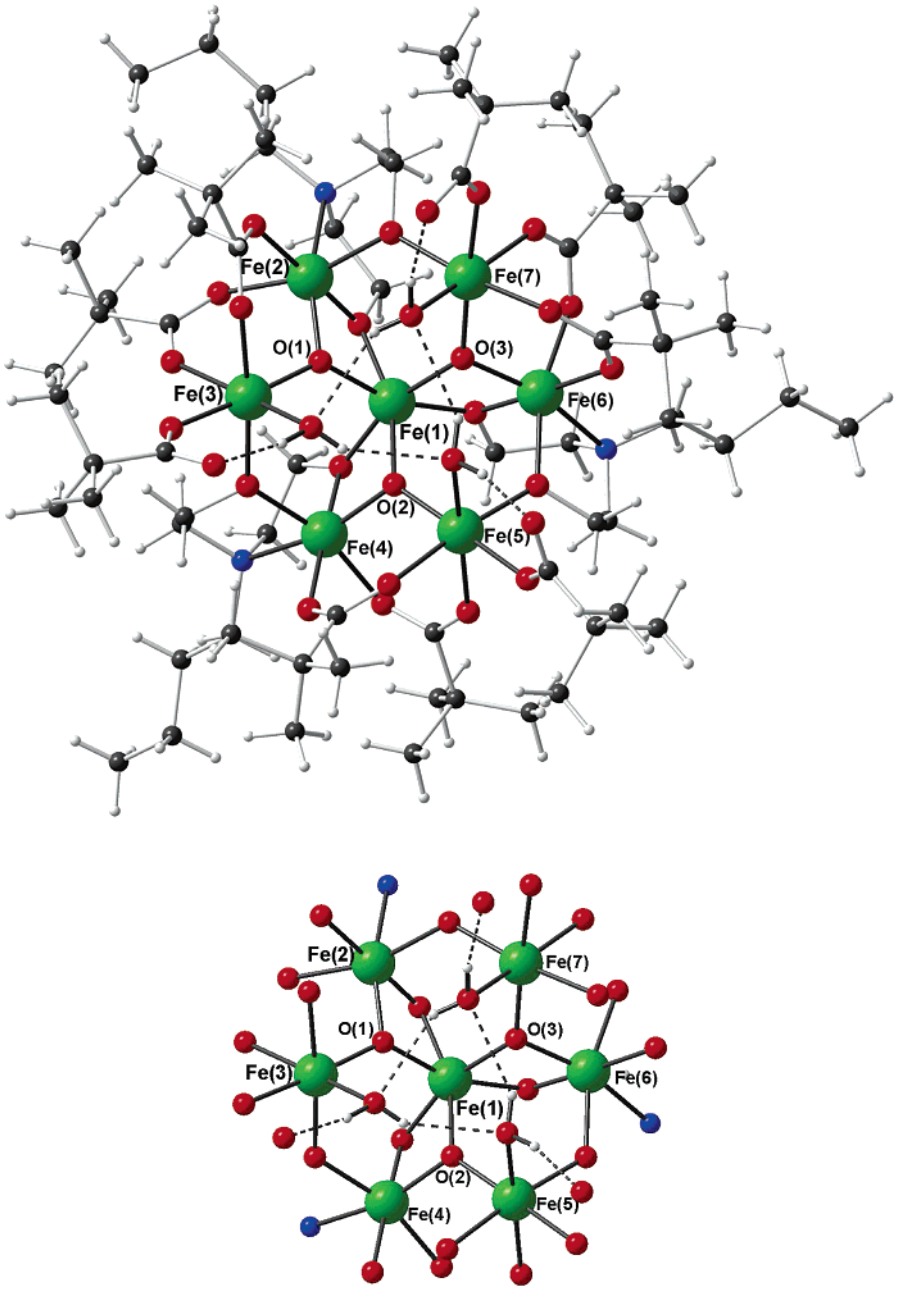

Figure 1. (Top) Molecular structure of **2** in the crystal. (Bottom) Core of **2**. Color code: green, Fe; red, O; blue, N; black, C; white, H.

1−**3** is rare for wheel-like diethanolamine complexes.[17] It is also directly related to that of the Fe_8 clusters **4** and **5** (see later). The structural features for the heptanuclear compounds **1**−**3** are described with reference to the detailed structural description of **2**. The structure of **2** consists of an $[Fe^{III}_7(\mu_3\text{-}O)_3]^{15+}$ core, with the peripheral ligation provided by six μ_2-bridging pivalate ligands, three bridging ^{n}Bu−$N(CH_2CH_2O)_2^{2-}$ ligands, three terminal pivalate ligands bonding in a unidentate fashion, and three terminal H_2O molecules coordinated to the Fe(3), Fe(5), and Fe(7) atoms. All Fe^{III} centers are hexacoordinated, displaying a distorted octahedral coordination sphere. Three types of Fe^{III} centers can be distinguished based on their coordination environment: (i) the central atom Fe(1), the coordination sites of which are occupied by three μ_3-O^{2-} and three μ_2-O^{2-} from the ethanolamine ligand to give an FeO_6 donor set; (ii) the peripheral Fe centers designated as type A [Fe(2), Fe(4), and Fe(6)] comprise an $FeNO_5$ coordination sphere made up of two μ_2-O^{2-} ethanolamine ligand O atoms, one ligand N, one μ_3-O^{2-}, and two O atoms from the bridging and terminal pivalate ligands, respectively; (iii) the peripheral Fe centers designated type B [Fe(3), Fe(5), are Fe(7)] comprise an FeO_6 chromophore with one μ_2-O^{2-} ligand O atom, one μ_3-O^{2-}, two O atoms from two bridging pivalate ligands, one O atom from a terminal pivalate ligand, and one O atom from a terminal aqua ligand. Hence, the pivalate ligands exhibit two different coordination modes; bidentate bridging and terminal monodentate and adjacent peripheral Fe centers are bridged, on the one hand, by a μ_3-O^{2-} connecting pairs of A and B centers to the central Fe and, on the other hand, by two bidentate pivalate ligands. Hydrogen bonding from the aqua ligands plays an important role in stabilizing the aggregates,

Table 2. Selected Bond Distances (Å) and Angles (deg) for Complex **2**

Bond Lengths			
Fe(1)−O(4)	1.9944(16)	Fe(4)−O(2)	1.8863(16)
Fe(1)−O(2)	2.0023(16)	Fe(4)−N(2)	2.236(2)
Fe(1)−O(1)	2.0066(16)	Fe(5)−O(2)	1.8577(16)
Fe(1)−O(3)	2.0085(16)	Fe(6)−O(3)	1.8819(15)
Fe(2)−O(1)	1.8878(16)	Fe(6)−N(3)	2.238(2)
Fe(2)−O(4)	1.9722(16)	Fe(7)−O(3)	1.8621(16)
Fe(2)−O(5)	2.0101(16)	Fe(1)···Fe(6)	2.9653(5)
Fe(2)−N(1)	2.243(2)	Fe(1)···Fe(4)	2.9686(5)
Fe(3)−O(1)	1.8597(15)	Fe(1)···Fe(2)	2.9751(5)
Bond Angles			
O(2)−Fe(1)−O(1)	90.34(6)	Fe(6)−Fe(1)−Fe(2)	119.037(16)
O(4)−Fe(1)−O(3)	102.57(7)	Fe(4)−Fe(1)−Fe(2)	118.271(15)
O(2)−Fe(1)−O(3)	90.51(7)	Fe(3)−O(1)−Fe(2)	118.93(8)
O(1)−Fe(1)−O(3)	89.68(6)	Fe(3)−O(1)−Fe(1)	134.57(9)
O(1)−Fe(2)−O(4)	81.21(7)	Fe(2)−O(1)−Fe(1)	99.58(7)
O(1)−Fe(2)−N(1)	59.57(7)	Fe(5)−O(2)−Fe(4)	119.13(9)
O(4)−Fe(2)−N(1)	78.93(7)	Fe(5)−O(2)−Fe(1)	134.90(8)
N(1)−Fe(2)−Fe(1)	117.89(5)	Fe(4)−O(2)−Fe(1)	99.49(7)
N(2)−Fe(4)−Fe(1)	117.86(6)	Fe(7)−O(3)−Fe(6)	119.37(8)
N(3)−Fe(6)−Fe(1)	118.95(5)	Fe(7)−O(3)−Fe(1)	134.03(8)
Fe(6)−Fe(1)−Fe(4)	119.168(15)	Fe(6)−O(3)−Fe(1)	99.27(7)

with each such ligand forming one hydrogen bond to the O atom of the next aqua ligand in a cyclic manner and the other H forming a hydrogen bond to the noncoordinated O atom of a monodentate pivalate, as illustrated in Figure 1.

Description of the Crystal Structures of 4 and 5. Complex **4** crystallizes in the space group $P2_1/n$, while the isostructural complex **5** crystallizes in the space group $C2/c$. The structure of **4** is shown in Figure 2. The core structure of **4** and **5** has been previously reported as occurring in only three compounds and is derived from that of **1**−**3**. The octanuclear motif occurs as one of the units of the core of the largest homometallic Fe^{III} cluster $[Fe_{22}]$,[26] in the Fe_8 cluster $[Fe^{III}_8O_3(O_2CPh)_9(tea)(teaH)_3]\cdot MeCN$,[16a] and in the Fe_8 cluster $[Fe^{III}_8O_3(\mu_4\text{-tea})(teaH)_3(O_2C(CH_2)Me)_6F_3]\cdot 0.5MeOH\cdot 0.5H_2O$ recently reported by Murray et al.[17] The core consists of eight Fe^{III} ions bridged by four μ_4-O^{2-} ions. It can be described as a central Fe_2 pair bridged by three oxide μ_4-O^{2-} ions, each of which also bridges an outer Fe_2 pair. These outer Fe pairs are not coplanar, and thus the outer six Fe ions do not form a flat wheel. Instead, the three outer Fe pairs are again arranged like the blades of a propeller, with the central pair now representing the axle or axis of the propeller. The Fe_8 structure can be regarded as derived from that of the Fe_7 aggregates by the addition of an {Fe^{III}-(tea)} moiety, in which the chelating O atoms of the $(tea)^{3-}$ ligand have coordinated to Fe(1) forming μ_2-O bridges, replacing the three aqua ligands as shown in Figure 2. Because the three μ_3-O ligands in **1**−**3** now also coordinate to the extra Fe center, they become μ_4-O^{2-} ligands. The Fe_8 structures are completed by the replacement of the terminal monodentate pivalates by azide (**4**) or thiocyanate (**5**) ligands. Two types of $teaH_3$ ligands are thus now present, three doubly deprotonated and one triply deprotonated.

Magnetic Properties of 1 and 2. Figure 3 shows the temperature dependence of χT and the magnetization curves at 1.8 K for three samples of compound **1**. Sample #1 was prepared by procedure A, and samples #2 and #3 were both prepared by procedure B but from different batches. The functional dependencies of the measured curves are very similar for all three samples, but the absolute values differ widely. Apparently, despite careful sample handling, for this material we faced problems in properly determining absolute magnetic values. Nevertheless, some conclusions concerning the magnetism in **1** can be drawn. At 250 K, the value of χT is in the range of 7−11 emu K mol^{-1} and much smaller than the value of 30.64 emu K mol^{-1} expected for seven noninteracting high-spin Fe^{III} ions (spin $^5/_2$, $g = 2$). This indicates very strong overall antiferromagnetic interactions in the cluster, as suggested also by the decrease of χT with temperature. At low temperatures, χT levels off at values of 3.5−6 emu K mol^{-1}, with a further steep drop at the very lowest temperatures. This behavior demonstrates a magnetic ground state of the cluster with a total spin of $S = 2$, $^5/_2$, or 3 (the expected χT values are 3.001, 4.377, or 6.002 emu K mol^{-1}, respectively, for $g = 2$). The steep drop in χT at the lowest temperatures could be due to zero-field splitting. The magnetic ground state is unambiguously confirmed by the magnetization curves at 1.8 K, which approach values of 2.3−3.8 $N_A\mu_B$ at high fields, suggesting a spin ground state in the range of $S = 1-2$.

Although the reason for the inconsistent absolute values of the magnetic curves is as yet unclear, the similarity of the curves for the three samples suggests that the actual number of magnetic molecules in the samples is somehow overestimated (one possibility could be, for example, that 20−50% of the clusters lack the central Fe ion, resulting in $S = 0$ and, hence, a nonmagnetic ground state of these clusters). With this assumption, the low-temperature χT value as well as the saturation magnetization m_{sat} can be determined by S and a scaling factor $n \leq 1$, which corrects for a smaller number of magnetic molecules in the samples ($\chi T = nS(S + 1)/2$; $m_{sat} = n(2S)$; $g = 2$). For the three samples, n will be different, but for each sample, the two values of n determined independently from χT and m_{sat} should agree for the correct spin ground state S. Indeed, assuming $S = ^5/_2$, the n values determined from χT and m_{sat} agree to within 5% for each of the three samples, while they differ by more than 17% assuming $S = 2$ and by more than 9% assuming $S = 3$ (and even worse for other S values). Thus, one can conclude that complex **1** experiences very strong overall antiferromagnetic interactions, resulting in a magnetic cluster ground state with a total spin that most likely is $S = ^5/_2$.

Figure 4 presents the temperature dependence of χT and the magnetization curve at 1.8 K for compound **2**. For this material, we also studied several samples prepared by either procedure A or B using different batches, but here the measurements agreed within experimental error for all samples. The magnetic behavior is similar to that observed for **1**. At 250 K, χT assumes a value of 6.2 emu K mol^{-1}, much smaller than the value of seven uncoupled $S = ^5/_2$ Fe^{III} ions, indicating very strong antiferromagnetic interactions. With decreasing temperature, χT decreases slightly, in agreement with the presence of strong antiferromagnetic interactions. At low temperatures, χT approaches a value of 4.4 emu K mol^{-1}, consistent with an $S = ^5/_2$ cluster ground state (4.375 emu K mol^{-1} for $g = 2$). At the very lowest temperatures, χT shows a slight upturn, which could be due

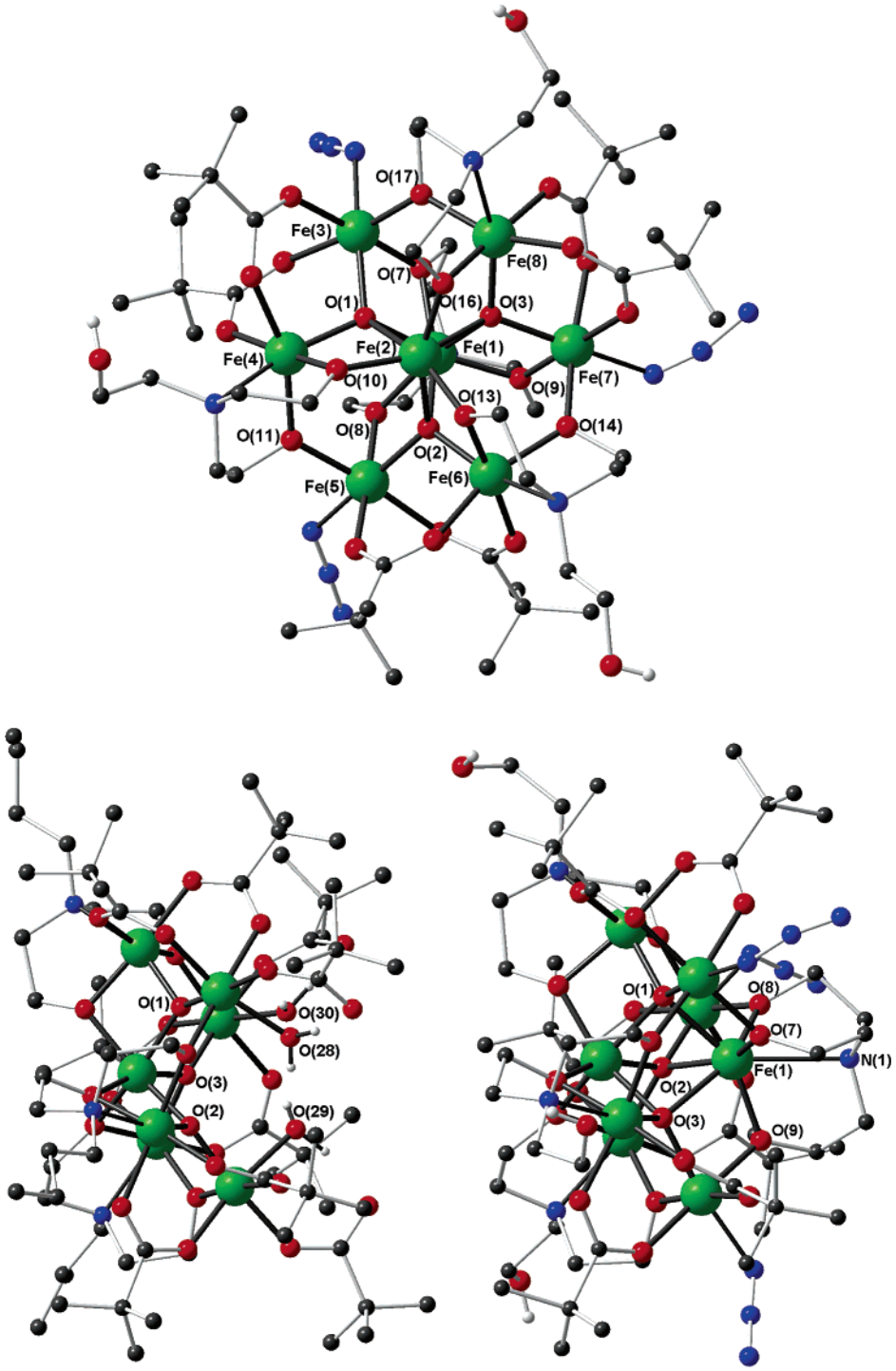

Figure 2. (Top) Molecular structure of **4** in the crystal. H atoms have been omitted for clarity. (Bottom) Side views of the cores in **2** (left) and **4** (right) illustrating their structural relationship.

to a small amount of paramagnetic impurities and/or very weak intermolecular magnetic interactions. The magnetization curve at 1.8 K unambiguously confirms a paramagnetic ground state with a total spin of $S = {}^5/_2$.

For compound **2**, we also measured a single crystal, as prepared by procedure C, with the magnetic field applied parallel to the (approximate) C_3 symmetry axis of the clusters and perpendicular to it. After completion of these measurements, the crystal was crushed into pieces to yield a polycrystalline sample and measured. The results for the temperature dependence of χT and the magnetization curves at 1.8 K are presented in Figure 5. The data clearly demonstrate a significant magnetic anisotropy of the easy-axis type due to zero-field splitting in the ground state of **2**. Figure 6 shows the magnetization curves of the crushed sample as measured at temperatures of 1.8, 2.4, 3.5, 5.0, and 7.5 K, plotted as function of B/T (B is the magnetic field). All curves collapse onto each other. Because of the very strong antiferromagnetic interactions in the cluster at temperatures below 50 K only the ground state is thermally

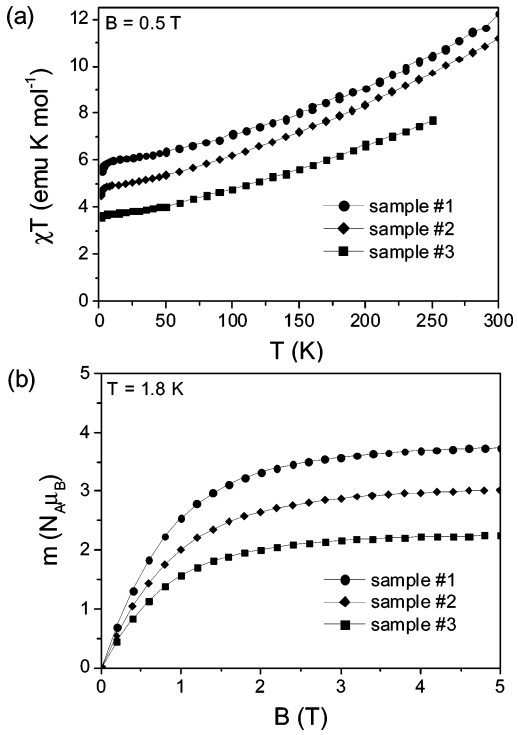

Figure 3. (a) Temperature dependence of the magnetic susceptibility, plotted as χT. (b) Low-temperature magnetization curves of three different polycrystalline samples of compound **1** (for the preparation details of the samples, see the text). The solid lines are guides to the eye.

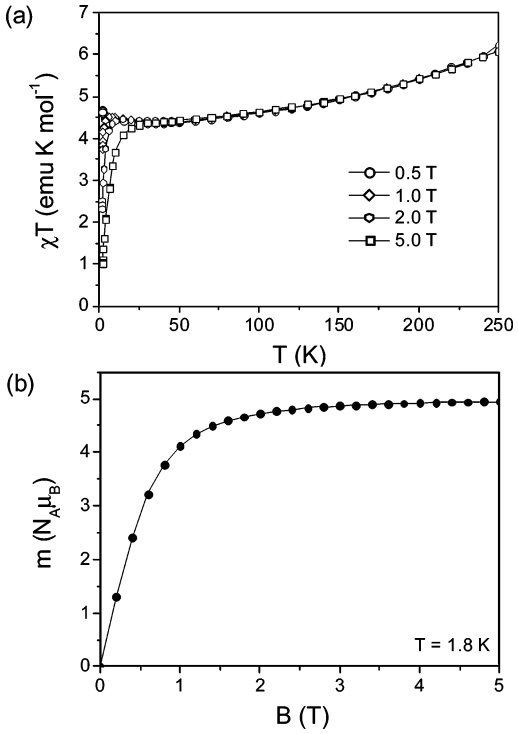

Figure 4. (a) Temperature dependence of the magnetic susceptibility, plotted as χT, as determined from different magnetic fields. (b) Low-temperature magnetization curve of a polycrystalline sample of compound **2**. The solid lines are guides to the eye.

populated, as confirmed by the near temperature independence of χT. Hence, the scaling behavior of the magnetization curves, which is usually interpreted as evidence for negligible

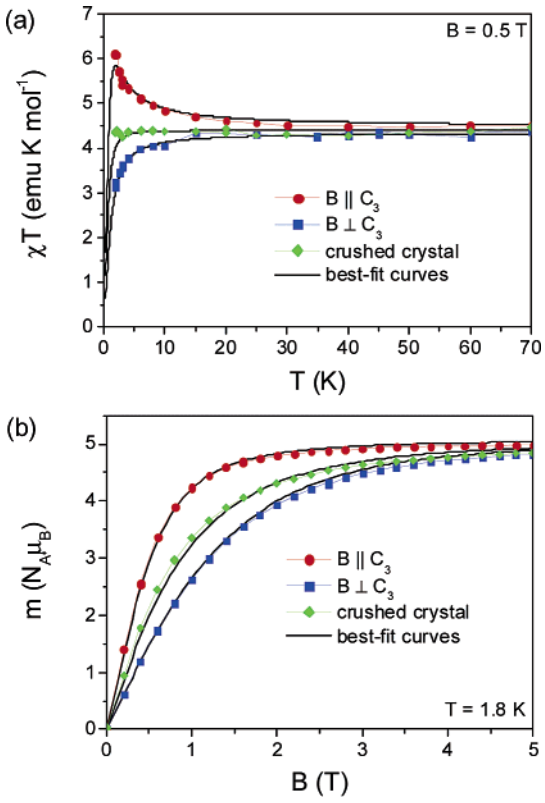

Figure 5. (a) Temperature dependence of the magnetic susceptibility, plotted as χT. (b) Low-temperature magnetization curves of a single-crystal sample of compound **2** for the magnetic field applied parallel and perpendicular to the cluster C_3-symmetry axis and for the crystal crushed into pieces. The colored solid lines are guides to the eye. The black lines represent the best-fit curves obtained from $\hat{H}_{S=5/2}$.

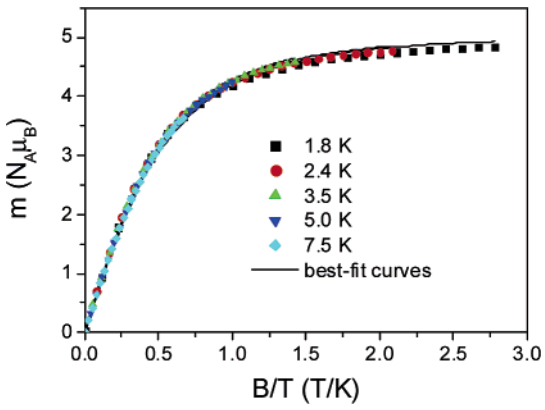

Figure 6. Magnetization curves at the indicated temperatures, plotted as a function of B/T, of a crushed single-crystal sample of compound **2**. The black lines (which are mostly covered by the data points) represent the best-fit curves obtained from $\hat{H}_{S=5/2}$ (the very small difference at the highest fields could be improved by assuming slightly smaller g factors in the calculations; it is recalled that the best-fit procedure used here included both the magnetization and χT curves; a fit to the magnetization curves alone would produce perfect-fitting curves).

zero-field splitting, is in seeming disagreement with the significant magnetic anisotropy visible in Figure 5, but, in fact, this is not the case, as will be shown below.

The low-temperature magnetism of **2** may be described as that of a single $S = {}^5/_2$ spin with easy-axis anisotropy, corresponding to the spin Hamiltonian

$$\hat{H}_{S=5/2} = D\left[\hat{S}_z^2 - \frac{1}{3}S(S+1)\right] + g_\perp \mu_B(\hat{S}_x B_x + \hat{S}_y B_y) + g_\parallel \mu_B \hat{S}_z B_z \quad (1)$$

where the *z* axis is perpendicular to the plane of the molecule. In view of the (approximate) 3-fold symmetry of the clusters, any orthorhombic magnetic anisotropy [corresponding to a term $E(\hat{S}_x^2 - \hat{S}_y^2)$ in the spin Hamiltonian] should be small and was neglected. All of the data for χT and the magnetization curves plotted in Figure 5 were least-squares-fitted simultaneously to the calculated curves obtained from diagonalizing eq 1. The best-fit results are displayed in Figure 5 as the black solid lines, and the agreement with the data is excellent. The parameters were obtained as $D = -0.43(2)$ K, $g_\perp = 1.99(2)$, and $g_\parallel = 2.02(2)$. Considering the accuracy of the determination of the weight of the sample, the values of the *g* factors are in perfect accord with the expectation for Fe^{III} ions. With these best-fit values, also the magnetization curves as a function of B/T were calculated for the appropriate temperatures. The results are plotted as black solid lines in Figure 6 and are in full agreement with the experiment. Hence, even with a small but significant magnetic anisotropy, an approximate scaling behavior is observed, which, in turn, implies that through a study of the deviation from scaling only rather large magnetic anisotropies may be detected.

During the preparation of this manuscript, a magnetic study of compound **1** appeared.[17] The reported χT and magnetization curves are essentially identical with those observed here for compound **2** (Figure 4), but the anisotropy parameters of the $S = {}^5/_2$ ground state were determined from powder electron paramagnetic resonance (EPR) measurements to be $D = +0.41$ K and $E/D = 0.21$. The magnitude of *D* is similar to our finding for compound **2** but of opposite sign (we carefully checked that our measurements cannot be explained with $D > 0$). Also, the large ratio of E/D reported for **1** is inconsistent with its crystallographic C_3 molecular symmetry. The reason for these discrepancies is unclear. Further studies such as single-crystal EPR measurements are required to clarify the situation.

Finally, the exchange-coupling situation in compound **2** along with the origin of the $S = {}^5/_2$ ground state can be discussed. This is of interest because of the spin frustration interactions between the Fe sites. Considering the exchange paths and the approximate 3-fold symmetry, the exchange model for **2** should include four different exchange interactions, J_1, J_2, J_3, and J_4 (see Figure 7). Although the slight deviation from the 3-fold symmetry will have some influence on the exchange integrals, the effects will be weak, and for a discussion of the general behavior, the assumption of a 3-fold symmetry is certainly a very good starting point; see also refs 9c and 30. The available data, however, do not allow for the determination of so many exchange constants (in particular, as they are very strong so that the temperature dependence of χT reflects just a few low-lying spin states). Hence, the simplified model with $J_1 = J_2 \equiv J_R$ and $J_3 = J_4 \equiv J_C$ was used, which is based on the rationale that the frustration in **2** originates from the competition between the exchange interactions on the ring of the outer Fe ions (J_1 and J_2) and those between the ring and the central ion (J_3 and J_4) and that this key element is correctly incorporated in the simplified model. The corresponding exchange Hamiltonian is given by

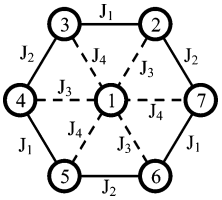

Figure 7. Exchange-coupling model.

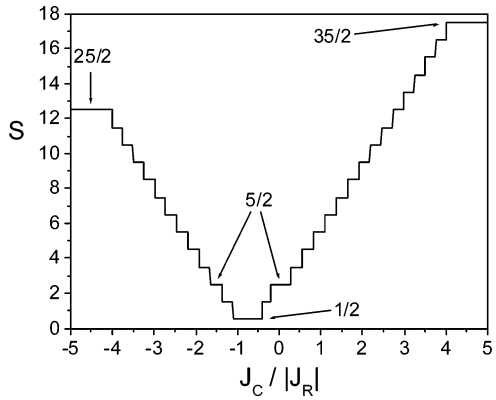

Figure 8. Total spin *S* of the ground state of the exchange model eq 2 as a function of $J_C/|J_R|$, assuming antiferromagnetic J_R.

$$\hat{H} = -J_R\left(\sum_{i=2}^{6} \hat{S}_i \cdot \hat{S}_{i+1} + \hat{S}_7 \cdot \hat{S}_2\right) - J_C(\hat{S}_2 + \hat{S}_3 + \hat{S}_4 + \hat{S}_5 + \hat{S}_6 + \hat{S}_7) \cdot \hat{S}_1 \quad (2)$$

which notably corresponds exactly to the heptanuclear species of the frustrated Heisenberg star introduced in ref 18. The energies of $\hat{H}$ are easily calculated, as has been noted already earlier,[18,31] with the spin-coupling scheme $\hat{S}_R = \hat{S}_2 + \hat{S}_3 + \hat{S}_4 + \hat{S}_5 + \hat{S}_6 + \hat{S}_7$, $\hat{S} = \hat{S}_R + \hat{S}_1$, and the energies $E_R(S_R,\alpha)$ of the Hamiltonian $\hat{H}_R = \sum_{i=2}^{6} \hat{S}_i \cdot \hat{S}_{i+1} + \hat{S}_7 \cdot \hat{S}_2$, which is related to the ring of the outer Fe ions (α is an additional quantum number for labeling of the different spin levels with equal S_R). The energies $E_R(S_R,\alpha)$ can easily be calculated numerically.[32] The energies $E(S,S_R,\alpha)$ of the spin states of $\hat{H}$ then simply become

$$E(S,S_R,\alpha) = -J_R E_R(S_R,\alpha) - \frac{J_C}{2}[S(S+1) - S_R(S_R+1) - S_7(S_7+1)] \quad (3)$$

In Figure 8, the total spin of the ground state of the exchange model eq 2 as a function of the exchange constant J_C between the Fe ions on the ring and the central Fe ion (an antiferromagnetic exchange constant J_R was assumed) is plotted. For strongly ferromagnetic values of J_C, $J_C/|J_R|$

(30) Waldmann, O.; Güdel, H. U. *Phys. Rev. B* **2005**, *72*, 094422.

(31) Waldmann, O. *Phys. Rev. B* **2000**, *61*, 6138.

(32) Gatteschi, D.; Pardi, L. *Gazz. Chim. Ital.* **1993**, *123*, 231.

> 4, the ferromagnetic configuration with all spins aligned parallel, and hence $S = {}^{35}/_2$, becomes the ground state. For strongly antiferromagnetic values of J_C, $J_C/|J_R| < -4$, a ferromagnetic configuration of the spins on the ring is realized, with the central spin oriented oppositely, and hence $S = 6 \times {}^5/_2 - {}^5/_2 = {}^{25}/_2$. A third unfrustrated spin configuration is obtained for small values of J_C, i.e., for $-0.19 < J_C/|J_R| < +0.27$, where a $S = {}^5/_2$ spin ground state is obtained. Here, the spins on the outer ring assume an antiferromagnetic configuration ($S_R = 0$) to which the central spin is coupled so weakly that it is not disturbed by the interaction J_C.

For all other values of J_C, frustration is apparently of great relevance, and with a proper choice of $J_C/|J_R|$, every spin state between $S = {}^1/_2$ and ${}^{35}/_2$ can be stabilized. The strongest frustration, signaled by the minimal spin ground state of $S = {}^1/_2$, is realized in the range $-1.10 < J_C/|J_R| < -0.40$. Interestingly, a further $S = {}^5/_2$ ground state, with a necessarily frustrated spin configuration, is obtained in the range $-1.65 < J_C/|J_R| < -1.38$. Hence, from the observation of an $S = {}^5/_2$ ground state in compound **2**, it is not possible to decide whether the unfrustrated configuration with $J_C \approx 0$ or the frustrated configuration with $J_C \approx -1.5|J_R|$ is realized. The temperature-dependent χT curve is of no help here because only the very lowest spin levels are involved in the weak upturn of χT at the higher temperatures, which for both configurations are $S = {}^3/_2$, ${}^5/_2$, and ${}^7/_2$ levels. Using eq 3 and the van Vleck formula, it is easy to calculate the magnetic susceptibility for any J_C and J_R, but the comparison with the experimental data did not yield any further insights despite the fact that the exchange constants are numerically large. From magnetostructural correlations, it was argued that for compound **1** the exchange interactions J_3 and J_4 (and, hence, also J_C) should be ferromagnetic,[13] which would imply the nonfrustrated $S = {}^5/_2$ ground-state configuration. More measurements, such as inelastic neutron scattering, would be needed to clarify the interesting exchange-coupling situation in **2**.

Conclusions

We have synthesized hepta- and octanuclear Fe^{III} clusters **1**−**5** presenting a rare topology. These complexes are an addition to a very limited number of this class of compounds described so far, with compound **3** representing the first example of a high-nuclearity Phdea-based complex reported to date. The nature of the side arm of the diethanolamine ligands has no influence on the core topology of the Fe^{III}_7 complexes. The synthetic approach employed in the preparation of **1**−**3** can be used to synthesize a variety of other compounds, which will be reported elsewhere.

Concerning the magnetism in compounds **1** and **2**, the presence of very strong intramolecular exchange interactions of overall antiferromagnetic sign can be concluded from the temperature profiles of the magnetic susceptibility. For **2**, the spin of the ground state was determined to be $S = {}^5/_2$ and single-crystal magnetic measurements revealed a uniaxial magnetic ansiotropy in the ground state of the easy-axis type with $D = -0.43(2)$ K. With respect to the exchange interactions in **2**, it has been shown that the $S = {}^5/_2$ ground state can be either due to a nonfrustrated situation, where the exchange couplings between the Fe^{III} ions on the outer ring and the central Fe^{III} ion are rather weak and below a certain threshold, or due to frustration with competing interactions on the ring and to the central ion. Further studies using complementary techniques such as inelastic neutron scattering are needed to resolve this ambiguity. From a general perspective, the disklike topology of homonuclear magnetic centers realized in compounds **1** and **2** exhibits close ties to the theoretical model of a frustrated Heisenberg star, which is one of the very few solvable models in the area of frustrated quantum-spin systems. Depending on the details of the exchange-coupling strengths, all spin ground states ranging from $S = {}^1/_2$ to ${}^{35}/_2$ can be realized in such a topology. Hence, a slight variation of the exchange interactions by, e.g., a chemical tuning can have pronounced effects on the spin ground state. This will be an attractive research topic for future work on odd-numbered disklike metal clusters.

Acknowledgment. This work was supported by the DFG (Grant SPP 1137 and Center for Functional Nanostructures), Alexander von Humboldt Stiftung (postdoctoral fellowship for V.M.), MAGMANet (Grant NMP3-CT-2005-515767), the EC-RTN-QUEMOLNA (Contract No. MRTN-CT-2003-504880), and the Swiss National Science Foundation.

Supporting Information Available: Crystallographic data for compounds **1**−**6** in CIF format and the structure of **6** with selected bond lengths and angles. This material is available free of charge via the Internet at http://pubs.acs.org. Crystallographic data have also been deposited with the Cambridge Crystallographic Data Centre under CCDC nos. 618914−618919 for compounds **1**−**6**. Copies of this information may be obtained free of charge from the Director, CCDC, 12 Union Road, Cambridge CB2 1EZ, U.K. (fax, +44-1223-336033; e-mail, deposit@ccdc.cam.ac.uk; Web site, http://www.ccdc.cam.ac.uk).

IC061650S